

Spatial Guilds in the Serengeti Food Web Revealed by a Bayesian Group Model

Edward B. Baskerville^{1,*}, Andy P. Dobson², Trevor Bedford^{1,3}, Stefano Allesina⁴, Mercedes Pascual^{1,3}

1 Department of Ecology and Evolutionary Biology, University of Michigan, Ann Arbor, Michigan, United States of America

2 Department of Ecology and Evolutionary Biology, Princeton University, Princeton, New Jersey, United States of America

3 Howard Hughes Medical Institute, University of Michigan, Ann Arbor, Michigan, United States of America

4 Department of Ecology and Evolution, Computation Institute, The University of Chicago, Chicago, Illinois, United States of America

* E-mail: ebaskerv@umich.edu

Abstract

Food webs, networks of feeding relationships among organisms, provide fundamental insights into mechanisms that determine ecosystem stability and persistence. Despite long-standing interest in the compartmental structure of food webs, past network analyses of food webs have been constrained by a standard definition of compartments, or modules, that requires many links within compartments and few links between them. Empirical analyses have been further limited by low-resolution data for primary producers. In this paper, we present a Bayesian computational method for identifying group structure in food webs using a flexible definition of a group that can describe both functional roles and standard compartments. The Serengeti ecosystem provides an opportunity to examine structure in a newly compiled food web that includes species-level resolution among plants, allowing us to address whether groups in the food web correspond to tightly-connected compartments or functional groups, and whether network structure reflects spatial or trophic organization, or a combination of the two. We have compiled the major mammalian and plant components of the Serengeti food web from published literature, and we infer its group structure using our method. We find that network structure corresponds to spatially distinct plant groups coupled at higher trophic levels by groups of herbivores, which are in turn coupled by carnivore groups. Thus the group structure of the Serengeti web represents a mixture of trophic guild structure and spatial patterns, in contrast to the standard compartments typically identified in ecological networks. From data consisting only of nodes and links, the group structure that emerges supports recent ideas on spatial coupling and energy channels in ecosystems that have been proposed as important for persistence. Our Bayesian approach provides a powerful, flexible framework for the study of network structure; we believe it will prove instrumental in a variety of biological contexts.

Introduction

Food webs, networks of feeding relationships in ecosystems, connect the biotic interactions among organisms with energy flows, thus linking together population dynamics, ecosystem function, and network topology. Ecologists have been using this powerful conceptual tool for more than a century [1–3]. One element of structure of particular relevance to large food webs is the subdivision of species into compartments or groups, a feature that has been proposed to contribute to food web stability by constraining the propagation of disturbances through a

network [4]. Although a large literature has considered the presence and dynamic significance of compartments in food webs, on the whole, evidence for the importance of compartments has been inconclusive [5–8]. In this literature, compartments are alternately referred to as modules, clusters, or “communities” [9], and are defined by high link density within groups and low link density between them.

Recent work with a probabilistic model considers a more flexible notion of groups, allowing link density to be high or low within any group or between any pair of groups [8]. Groups can thus represent compartments in the previous sense, but can

also represent trophic guilds or roles [10, 11], sets of species that feed on, and are fed on, by similar sets of species. By fitting models of this type to data, the dominant topological pattern in the network can be found, which may include (spatial) compartments, or trophic guilds, or some combination of the two. The initial application of this model to empirical food webs from different ecosystems has revealed a predominance of trophic guilds rather than compartments [8].

Two major challenges limit the application of this model in resolving the group structure of large food webs and interpreting its biological basis. First, most food webs have poor resolution of primary producers; plants in terrestrial systems and phytoplankton in aquatic ones are typically represented by a few nodes that are highly aggregated taxonomically. This is unfortunate, because their position at the base of a food web means that primary producers are essential for understanding how the web is spatially organized, and how this spatial organization percolates up through the trophic relationships of other species. Fully resolved primary producers are also essential in examining how the structure of other trophic levels cuts across their spatial distribution, and, in so doing, couples different habitats.

Second, some technical problems have hindered the use of probabilistic models in analyzing group structure. Early food web models served as null models for food web structure and were tested by generating model webs and comparing summary statistics against data from real webs [12, 13]. More recently, a more rigorous approach for measuring the goodness of fit of a model has been provided by maximum likelihood and model selection [8, 14]; two problems still remain within this framework. One is technical: standard model-selection criteria are not applicable to “discrete parameters” such as group membership. The second problem is more fundamental: there are many almost equally good arrangements, and it is desirable to extract information not just from a single best arrangement, but also from the rest of the ensemble.

The Bayesian approach is gaining popularity in ecological modeling due to the philosophical and conceptual appeal of explicitly considering uncertainty in parameter estimation as well as its methodological flexibility [15]. This approach is es-

pecially well-suited for handling uncertainty in complex food web models, and allows us to overcome the limitations of the previous implementation of the group model. In network inference, there are only a few examples of complete Bayesian models [16, 17] and a few examples of MCMC for maximum-likelihood inference [18, 19], but Bayesian inference in phylogenetics has been long established [20, 21], and provides a clear methodological analogue.

In this paper, we address the group structure of a newly assembled food web for the mammals and plants of the Serengeti grassland ecosystem of Tanzania; we use a new and novel approach to the identification of groups based on Bayesian inference. We specifically ask whether the structure that emerges reflects the underlying spatial dimension, as delineated by the different plant communities that characterize different sub-habitats within the ecosystem, or whether it is determined by trophic dimensions in the form of species guilds that share functional roles.

The Serengeti food web is emerging as the most highly resolved terrestrial web to date [22]. The Serengeti has been studied as an integrated ecosystem for almost five decades [23–25], and because of widespread popular familiarity with the consumer-resource dynamics of lions, hyenas, wildebeest, zebra and grasses, it provides a strong intuitive test for probabilistic food web models. Most importantly, at the primary producer level, the Serengeti food web includes a number of distinct grass and woodland plant communities on different soils and across a rainfall gradient [26]. The sequential and well-documented changes in the underlying plant diversity allows us to examine the extent to which grassland communities define network topology at higher trophic levels. The high resolution of the species that comprise the mammal and plant communities of the ecosystem allow us to address the role of space in the group structure of the food web.

From a complex network of only nodes and links that represent species and their interactions, the groups that emerge from an otherwise blind classification of species make remarkable biological sense. We find that the group structure identified in the Serengeti food web represents a mixture of trophic guild structure and spatial patterns, an arrangement that differs significantly from the compartmental structure typically identified in ecological

networks.

Results/Discussion

Bayesian Inference and Model Selection for Food Webs

Probabilistic Models for Food Webs

In this paper, we use probabilistic modeling as a tool for formalizing hypotheses about food web structure. We treat a food web, an observed network of who eats whom in an ecosystem, as data. We start with the basic question: assuming a probabilistic model of food web structure, what is the probability of observing this particular real-world food web? This probability is referred to as the *likelihood* of observing the data, given model parameters. In a maximum-likelihood framework, the mechanical part of the inference process is to find the set of model parameters that makes the likelihood as great as possible, with the interpretation that this represents the best point estimate of the underlying process.

We begin with the group model of Allesina and Pascual [8], which was originally treated in a maximum-likelihood framework. Conceptually, this model encodes the simple hypothesis that species can be divided into groups, and species in the same group have statistically similar behavior: they tend to consume species in certain groups and tend to be consumed by species in certain groups. Specifically, the probability that a species belonging to group i is eaten by a species belonging to group j is given by p_{ij} , and conversely, the probability of a link being absent is $(1 - p_{ij})$. If there are K groups, then a matrix \mathbf{P} of K^2 link probabilities is required to completely describe the relationships among all groups. The likelihood for the whole network is the product over all pairs of species of the probability of a link being present (if present) or absent (if absent). In the statistical literature, this model structure is known as a stochastic block model [27]. The assignment of species to groups is also an unobserved parameter in this model, which adds a layer of difficulty to parameter estimation. For example, in a network of 100 species, there are approximately 5×10^{115} different ways to partition the network into groups (see Methods). That is, if you had a computer that could process 10^{80} partitions (as many

partitions as there are atoms in the universe) every femtosecond (10^{-15} s), it would take 1.5×10^{13} years to process them all. (By comparison, the universe is only 1.4×10^{10} years old.)

The group model allows for a more flexible definition of groups than standard approaches to network clustering, which find groups that have large numbers of internal connections and relatively few connections between groups [9]. Because each p_{ij} parameter may take any value between 0 and 1, good model fits may result from other relationships, such as high link density between groups and low link density within groups, and may accommodate different relationships in different parts of the network. In general, the best-fitting partitions will try to maximize or minimize the number of links within specific groups and between specific pairs of groups.

Bayesian Inference and Priors for the Group Model

In a Bayesian framework, rules of probability are taken to govern both the data and model parameters. Rather than finding the set of parameter values that maximize the likelihood, the goal becomes to estimate a probability distribution over parameters based on observed data. In this way, we can directly quantify the uncertainty in our parameters in terms of probabilities. This permits questions such as: what is the probability that a parameter lies in a particular range? The name ‘‘Bayesian’’ comes from Bayes’ rule, which tells us how to use conditional probability statements to infer a *posterior* distribution, in this case, the probability distribution over parameter values conditional on having observed the data, $\Pr(\theta|D)$. If we are dealing entirely with discrete probability distributions, Bayes’ rule takes its most intuitive form:

$$\Pr(\theta|D) = \frac{\Pr(\theta)\Pr(D|\theta)}{\Pr(D)}. \quad (1)$$

The numerator of the right-hand-side is the probability of producing the data from the given parameters: the *prior* probability of those parameters, $\Pr(\theta)$, times the probability of producing the data given those parameters, $\Pr(D|\theta)$, the likelihood. The denominator is the *marginal* probability of observing the data unconditional on the particular parameter values at play, which is simply the

sum of the probabilities of all the different ways of producing the data using all possible parameter values, $\Pr(D) = \sum_{\theta} \Pr(\theta)\Pr(D|\theta)$. In other words, in order to calculate the posterior probability of parameters θ , we add up all the different ways of producing the data weighted by their probability, and then calculate what fraction of that probability came from parameters θ . From here, we will write these quantities in more general notation, suitable for a mix of discrete and continuous probability distributions:

$$f(\theta|D) = \frac{f(\theta)f(D|\theta)}{\int_{\theta} f(\theta)f(D|\theta) d\theta} \quad (2)$$

where the integral sign represents a multiple integral over discrete and continuous parameters.

In the Bayesian framework, the model includes not only the formulation of the likelihood but also a prior distribution over parameters. With the group model, this means defining a prior distribution over both link probabilities and arrangements into groups (“partitions”). In general, priors may incorporate informed knowledge about the system, but in this case we simply use them to encode different variants of the same basic model. We use two distributions for partitions and two distributions for link probabilities, which are combined to form four different model variants.

The two alternative distributions for elements p_{ij} of the link probability matrix \mathbf{P} are (1) a uniform distribution between 0 and 1, and (2) a beta distribution with shape parameters α and β , which are in turn governed by exponential distributions with mean 1. With α and β fixed at their means, alternative (2) reduces to a uniform distribution; at other values, the distribution may take a uniform, convex, concave, or skewed shape. Alternative (2) is thus structured hierarchically, with exponential *hyperpriors* for α and β governing the beta prior for elements of \mathbf{P} .

For partitions, we consider (1) a uniform distribution and (2) a distribution generated by the Dirichlet process, sometimes referred to as the “Chinese restaurant process” [28]. Alternative (2) is controlled by an aggregation parameter χ that is in turn drawn from an exponential distribution with mean 1. The uniform distribution assigns equal prior probability to each possible partition, irrespective of the number of groups. Because there

are far more ways to partition the network at an intermediate, but relatively high, number of groups, the uniform prior implicitly biases the model toward that number. For example, in the Serengeti food web, there are 170 nodes, yielding an *a priori* expectation of 43.8 groups. In contrast, the hierarchically structured Dirichlet process prior provides flexibility via the aggregation parameter χ . When χ is large, partitions tend to have many small groups; when χ is small, partitions tend to have fewer groups, with a skewed group size distribution.

We also consider two simple models without groups as null comparisons: (1) a directed random graph model (i.e., one group) with a uniform prior on a single link probability parameter p , and (2) a fully parameterized model, with each species in its own group (and a 170×170 link probability parameter matrix \mathbf{P} , also with a uniform link probability prior.

For a fuller discussion of models and prior distributions, in particular the properties of the distribution generated by the Dirichlet process, see Methods.

Bayesian Model Selection via Marginal Likelihood

The Bayesian framework provides a natural way to make probabilistic inferences based on a particular model. However, we also want to be able to choose between different models by quantifying their relative goodness of fit. One approach to Bayesian model selection can be framed directly in terms of Bayes’ rule, mirroring the process for estimating the posterior distribution over parameters for a single model.

Consider two models, M_1 and M_2 , to which we assign prior weight $\Pr(M_1)$ and $\Pr(M_2)$. After the data has been observed, we can calculate the posterior probability of the models using Bayes’ rule:

$$\Pr(M_1|D) = \frac{\Pr(M_1)\Pr(D|M_1)}{\Pr(D)}, \quad (3)$$

$$\Pr(M_2|D) = \frac{\Pr(M_2)\Pr(D|M_2)}{\Pr(D)}, \quad (4)$$

where the denominator is equal to the probability of observing the data unconditional of the particular model at play, $\Pr(D) =$

$\Pr(M_1)P(D|M_1) + \Pr(M_2)P(D|M_2)$. The probabilities $\Pr(D|M_1) = \int_{\theta_1} f(\theta_1)f(D|\theta_1) d\theta_1$ and $\Pr(D|M_2) = \int_{\theta_2} f(\theta_2)f(D|\theta_2) d\theta_2$ are the marginal likelihoods of the two models, corresponding to the denominator in Equation 2. If we give the two models equal prior weight, then the relative posterior weight of the two models is simply given by the marginal likelihoods. This reasoning extends naturally to any number of models.

The ratio of the marginal likelihoods is often called the Bayes factor [29–31], and is equal to the posterior odds ratio of the two models, assuming equal prior weight:

$$B_{12} = \frac{\Pr(D|M_1)}{\Pr(D|M_2)} \quad (5)$$

The Bayes factor provides a convenient way to compare models: if $B_{12} = 10$, then we consider support for model M_1 to be ten times stronger than model M_2 . In AIC-based model selection, the Bayes factor is analogous to a ratio of Akaike weights [32].

Consensus Partitions

The output of an MCMC simulation includes a long sequence of network partitions representing draws from the posterior distribution over partitions. As these partitions are potentially all distinct from each other, but represent similar tendencies of species to be grouped together, it is useful to try to summarize the information contained in all the samples in a more compact form. One approach is to construct a pairwise group-membership matrix for species in the food web, with entries equal to the posterior probability that two species are in the same group. A visual representation of this matrix can illuminate the group structure, and a consensus partition can then be constructed from this matrix using a simple clustering algorithm. (For more details, see Methods.)

Bayesian analysis of the Serengeti food web

The Serengeti Data Set

We compiled the food web from published accounts of feeding links in the literature [26, 33–45].

The compiled Serengeti food web (Tables S1 and S2 and Figure 1) consists of $L = 667$

feeding links among $S = 170$ species (136 plants, 25 herbivores, and 9 carnivores). 550 of the links are herbivorous, and 117 are predatory. The fraction of all possible links or connectance ($C = L/S^2$), ignoring all biological constraints, is equal to 0.0231.

Performance of Model Variants

We find unequivocal support for the use of group-based models in describing the Serengeti food web. Models with group structure have vastly greater marginal likelihoods than simple null models that ignore group structure (Table 1). Furthermore, the use of both the Dirichlet process prior for network partitions and the beta prior for link probability parameters vastly improved the fit of the basic model. The best model variant as measured by marginal likelihood included both the beta prior on link probabilities and the Dirichlet process prior on partitions. The next best variant included a uniform partition prior and beta link probability prior, followed by the variant with Dirichlet process prior and uniform link probability prior. The strongest variant surpassed its closest competitor by 106 log-orders in likelihood and surpassed the model with two uniform priors by 470 log-orders in likelihood, providing unequivocal support for including both flexible priors in the model specification. Accordingly, in the remaining analysis we consider only the best model variant.

Identification of Model Parameters

The posterior mean number of groups K is 14.9 (95% credible interval 12, 18), and the mean value of the Dirichlet process parameter χ is 3.2 (1.6, 5.3) (Figure 2). The prior expectation of χ was 1.0 and the prior expectation of K was 5.4. The finding of posterior values substantially greater than prior values strongly supports the presence of detailed group structure in the Serengeti food web.

Mean values for beta distribution parameters are $\alpha = 0.046$ (0.029, 0.068) and $\beta = 0.89$ (0.50, 1.43) (Figure S2). The corresponding beta prior has support concentrated near 0, since most species do not feed on most other species (Figure S3).

Groups Identified in the Serengeti Food Web

The structure of the Serengeti food web is best represented by groups containing trophically similar species, subdivided by specialization on different components of prey species, with plant species corresponding to spatially distinct habitats. The best consensus partition, with 16 groups, is shown in Table 2. There are 6 groups of plant species (groups 11–16), 7 groups of herbivore species (groups 4–10) and 3 groups of carnivores species (groups 1–3). On average, plant groups contain more species than herbivore and carnivore groups (22.7, 3.6 and 3.0, respectively). As evident in the pairwise group-membership matrix (Figure 3), the carnivore and herbivore groups are well-defined, including several individual species or pairs of species with distinct diets. Plant groups demonstrate mild overlap, indicating a partially hierarchical relationship between smaller groups and larger groups.

Figures 4, 6, and 5 show three alternate views of the food web, organized by the 16-group consensus partition. Groups 11–13, 14–15, and 16 consist of plants located in grassland, woodland, and kopje habitat, respectively. Group 11 includes short grasses that are grazed by a wide variety of species, distinguished from group 12, which includes short grasses fed on only by the large grazers (4). The 1-species groups (2, golden jackal *Canis aureus*; 6, African buffalo *Syncerus caffer*; 8, agama lizard *Agama planiceps*; 10, elephant *Loxodonta africana*; and 13, *Microchloa kunthii*) represent individual species with distinct diets or consumers.

Plant groups are coupled by groups of herbivores, which are in turn coupled by groups of carnivores. Large migratory grazers (4, wildebeest, zebra, and gazelles) feed primarily on plant groups consisting of grasses (11 and 12), and are the exclusive consumers of a group of grasses adapted to seasonal rainfall on sandy or volcanic soils (12) that dominate the short-grass plains in the southern part of the ecosystem. Herbivores feeding in the longer grasslands and woodlands and in riparian habitats (group 5) couple the first grass group (11) with woodland plants (group 14), which are also consumed to a lesser extent by the large grazers. The hyraxes (group 7) and group 9 (giraffe, olive baboon, and dik-dik) couple kopje habitat (group 16) with both woodland and grassland plants. At the highest trophic level, the large carnivores (1) inte-

grate across all the herbivore groups; smaller carnivores (2, 3) show more specialized diets, reflecting the more distinct habitats in which they are usually found.

Discussion

Spatial Guilds in the Serengeti Food Web

In order to analyze the group structure of the Serengeti food web, we used a flexible Bayesian model of network structure that includes no biological information aside from a set of nodes representing species and links representing their interactions. The groups that emerge from an otherwise blind classification of species make remarkable biological sense. Species are divided into trophic guilds that reveal a clear relationship between the spatial organization of plant, herbivore, and carnivore groups and the structure of the network. At the coarsest scale, the groups in the Serengeti food web correspond to carnivores, herbivores, and plants. The further subdivisions that emerge within carnivores, herbivores, and plants reveal a spatial dimension to feeding structure that is only evident because of high species resolution at the plant level. Ultimately, the group structure we have derived mirrors the flow of energy up the food web from different spatial locations, with herbivores integrating spatially separated groups of plants, and carnivores integrating spatially widespread herbivores. Although the addition of birds, reptiles, invertebrates, and pathogens will certainly add a significant number of new groups, we do not expect them to significantly modify the derived structure for the mammal and plant community. Nor will they modify the larger tendency for groups to be assembled in ways that reflect the underlying spatial and trophic structure of the species in the web.

Recently, interesting theoretical and empirical work has highlighted the relationship between observed patterns of food-web structure and energy flow that seemingly mirrors the trophic guild structure in the Serengeti. Rooney and colleagues [46] give evidence that real ecosystems may be dominated by nested sets of fast and slow “energy channels,” each of which represents a food chain of trophic guilds. They suggest that this pattern may have a strong stabilizing effect, based on theoretical work by McCann on spatially coupled food webs

[47]. The group structure for the Serengeti web that emerges from our analysis supports a pattern of spatial coupling at multiple trophic levels: the grasslands have very high turnover rates compared to those of the kopjes and woodlands. This suggests a similar pattern of fast and slow energy channels to those described by Rooney and colleagues, with fast energy flow up through the highly seasonal but very productive grasses of the short-grass plains. These are almost completely consumed by wildebeest and zebra during their peak calving season, which are then in turn consumed by large predators (lions and hyenas). In contrast, the resident herbivore species living on kopjes or in the woodlands reproduce at slower rates and are consumed less frequently by large carnivores, except during the time when they are unable to feed on migratory wildebeest and zebra. The group model and the inference approach presented here allow the examination of the dynamical consequences of this type of structure to be fully rooted in an empirical pattern, complementing more theoretical considerations of its central importance for preserving biodiversity [47].

These patterns emerge directly from the topology of the food web without being explicitly labeled as different habitats upfront as was done in previous empirical work [46], showing that topological analysis can reveal structures that may be very significant for food-web dynamics. They are subtly different, however, from the proposed pure fast and slow chains, in that they incorporate the migration of the keystone species in the ecosystem, so the fastest energy chain is seasonally ephemeral and may only operate for three to four months in any year. We suspect that even within the sub-habitats of kopjes and woodlands there are similarly nested faster and slower chains that involve species for which we are still collating data (e.g., birds, small mammals, and insects).

Bayesian Analysis of Food-Web Structure

In this paper, we used a probabilistic model to analyze the structure of a single food web, an approach we have seen in only one other study based on a probabilistic version of the niche model [19]. This approach has proved fruitful in Bayesian phylogenetics, where the combinatorial challenges are similar. Moreover, we view the group model as only a starting point for richer modeling efforts to help

identify relevant processes that influence the structure of ecological communities.

In fact, the Bayesian approach described here provides a powerful general framework for encoding hypotheses about the structure of food webs and comparing models against each other, and we see it as a natural next step in the current trend of representing food-web models in a common way. Simple abstract models such as the niche model and the group model used here act as proxies for the high-dimensional trait space that determines feeding relationships in an ecosystem. The identification of actual traits that correspond to groups (or niche dimensions) is another valuable direction, so far followed primarily by finding correlations between compartments/groups [48] or niche values [13] and traits such as body size or phylogenetic relatedness. Another approach is to directly incorporate these traits into the probabilistic models, either as model predictors or as informed priors. Both kinds of analyses are valuable, but the second kind becomes more approachable in a general Bayesian modeling framework.

The use of flexible hierarchical priors for model parameters is one straightforward innovation possible in the Bayesian framework. The number of groups identified by the model increases dramatically with the use of a flexible beta prior distribution for link probability parameters. In that model variant, we effectively introduce two degrees of freedom to the model (the beta distribution parameters) but dramatically reduce the effective degrees of freedom of the link probability parameters. Note that we properly penalize parameters by using the marginal likelihood for model selection, so that the model selection represents a balance between goodness of fit and model complexity. Moreover, this structure makes intuitive sense: since most link probability parameters are simply zero, they should not be penalized. An alternate approach is to remove and add parameters to the model, but this hierarchical technique is much easier to implement in practice.

Advanced Markov-chain Monte Carlo methods make it possible to accurately estimate marginal likelihoods for probabilistic network models. Unlike information criteria such as AIC, BIC, or DIC, an accurate estimate of the marginal likelihood provides a direct measurement of goodness of fit that

takes into account the degrees of freedom in a model without making any asymptotic assumptions about parameter distributions [49], and can handle discrete parameters such as partitioning into groups that are not properly handled by AIC and BIC.

The Bayesian approach also serves as a means to avoid fundamental issues inherent in network models with a large parameter space. In a recent study, Good and colleagues [50] examined the properties of module-finding in networks using the pervasive modularity-maximization approach [51], finding that even in relatively small networks a large number of good solutions exist. A maximization algorithm is thus guaranteed to find a single local maximum of many—possibly even the best one, but certainly not one that captures the full range of good solutions. This problem arises whether the quantity to be maximized is a heuristic such as modularity or a likelihood value. The group model and other parameter-rich models presumably suffer from similar degeneracy problems. In the present case, we find that every partition sampled from the posterior distribution for the best-fitting group model variant is unique. Although MCMC sampling cannot reproduce the full posterior distribution, it is an important step in the right direction. Philosophical arguments aside, one of the main reasons for maximizing likelihood or modularity is simply that a single solution is far more tractable than a distribution. The consensus partitioning heuris-

tic used here is one attempt at recovering a simpler object of study (see Methods); more sophisticated approaches will be welcomed.

The group model, based on the simple notion that groups of species may have similar feeding relationships to other groups, reveals that trophic guilds are the topologically dominant type of group in the Serengeti food web. The model also reveals an interesting relationship between spatial structure and network structure that corroborates recent ideas on spatial coupling in food webs. A theoretical study with a dynamical model suggests that this type of structure may contribute to ‘stability’ in the sense of the persistence of species [47]. We are now in a position to examine different aspects of stability, including robustness to secondary extinctions, based on structures directly inferred from empirical networks. Although the Bayesian modeling approach is not new to network analysis in general [16, 17], it remains relatively rare. The Bayesian group model, and, more importantly, the general framework for modeling and model selection, naturally extend to other kinds of biological networks, such as metabolic and regulatory networks [52] and networks describing other ecological interactions such as pollination [53]. We advocate this framework as a way to build stronger ties between hypothesis formulation, model building, and data analysis.

Methods

Group Model

We use as a starting point the group model of Allesina and Pascual [8], in which a network of N nodes is partitioned into K groups. The groups to which a potential prey and to which a potential predator belong completely determine the probability that a feeding relationship exists between them. The assignment of species to groups is given by the vector $\mathbf{G} = (g_1, \dots, g_n)$, with $g_i \in \{1, \dots, K\}$. We refer to this assignment as a set ‘partition,’ in keeping with standard mathematical terminology. The probability that a species assigned to group i is consumed by a species assigned to group j is equal to p_{ij} . This gives a matrix \mathbf{P} of K^2 probabilities, containing the probabilities of observing directed links between members of each pair of groups, and within members of each group.

If we take \mathbf{A} to be the directed adjacency matrix of a network, with entries a_{ij} equal to 1 if a link exists from node i to node j , 0 otherwise, then the probability of the network being generated by partition

\mathbf{G} and link probabilities \mathbf{P} is given by

$$f(\mathbf{A}|\mathbf{G}, \mathbf{P}) = \prod_{i=1}^K \prod_{j=1}^K p_{ij}^{Y_{ij}} (1 - p_{ij})^{Z_{ij}}, \quad (6)$$

where Y_{ij} and Z_{ij} are the number of 1-entries and 0-entries in the submatrix of \mathbf{A} containing entries from rows r satisfying $g_r = i$ and columns c satisfying $g_c = j$.

In the simplest case, all nodes are assigned to the same group, and the likelihood simplifies to

$$f(\mathbf{A}|p) = p^Y (1 - p)^Z \quad (7)$$

where Y and Z are the total number of 1-entries and 0-entries in \mathbf{A} .

In order to use the group model for Bayesian inference, we want to infer the posterior distribution over partitions and parameters,

$$f(\mathbf{G}, \mathbf{P}|\mathbf{A}) \propto f(\mathbf{G}, \mathbf{P})f(\mathbf{A}|\mathbf{G}, \mathbf{P}). \quad (8)$$

This requires specifying a prior distribution over partitions \mathbf{G} and link probabilities \mathbf{P} . We consider two priors over \mathbf{G} and two priors over \mathbf{P} .

Model Priors

Priors for Partitions

The simplest prior over partitions assigns equal probability to each possible assignment of nodes into groups. For a network of N nodes, the number of possible partitions is given by the N th Bell number,

$$\mathcal{B}(N) = \sum_{K=1}^N \mathcal{S}_2(N, K), \quad (9)$$

where $\mathcal{S}_2(N, K)$ is the Stirling number of the second kind, the number of ways to partition N objects into exactly K groups,

$$\mathcal{S}_2(N, K) = \frac{1}{K!} \sum_{j=0}^K (-1)^{K-j} \binom{K}{j} j^N. \quad (10)$$

Therefore, the prior probability of a particular partition is uniform across all possible partitions

$$f(\mathbf{G}) = \frac{1}{\mathcal{B}(N)}, \quad (11)$$

and the prior probability of having exactly K groups is

$$f(K) = \frac{\mathcal{S}_2(N, K)}{\mathcal{B}(N)}. \quad (12)$$

For partitions, the choice of a uniform prior, although simple, includes hidden assumptions. In particular, there are far more possible partitions for an intermediate number of groups than a small or large number, so the prior will implicitly bias results toward that number. For example, with 100 nodes, the distribution is peaked at $K = 28$ (Figure S1).

An alternate prior for partitioning objects into groups comes from the Dirichlet process, also known

as the ‘‘Chinese restaurant process,’’ which is becoming a standard Bayesian prior for related problems [28, 54, 55]. Consider a restaurant with an infinitely large number of infinitely large tables, all initially empty. The first patron sits alone at the first table, and subsequent patrons may either sit at an occupied table or a new table. They choose occupied tables with weight equal to the number of current occupants, or a new table with weight equal to an aggregation parameter χ . For example, the second patron will sit at the same table as the first patron with probability $1/(1 + \chi)$. In fact, because the process is *exchangeable*, the probability of any pair of patrons sitting at the table is also $1/(1 + \chi)$. If χ is small, there will tend to be a small number of occupied tables and a skewed distribution of table sizes; if χ is large, there will be a larger number of tables occupied by few patrons.

Interpreting tables of patrons as groups of nodes, under the Dirichlet process the prior probability of a particular partition \mathbf{G} is

$$f(\mathbf{G}|\chi) = \chi^K \frac{\prod_{j=1}^K (\eta_j - 1)!}{\prod_{i=1}^N (\chi + i - 1)}, \quad (13)$$

where N is the number of nodes in the network, K is the number of groups in the partition, and η_j is the number of nodes in group j . The prior probability of K groups is

$$f(K|\chi) = \frac{|\mathcal{S}_1(N, K)|\chi^K}{\prod_{i=1}^N (\chi + i - 1)}, \quad (14)$$

where $\mathcal{S}_1(N, K)$ is a Stirling number of the first kind, equal to the coefficients on x_K in the expansion $x(x-1)(x-2)\dots(x-K+1)$.

Rather than choosing a fixed value of χ for the prior, we give χ an exponential hyperprior distribution with mean 1:

$$f(\chi) = e^{-\chi} \quad \chi \geq 0. \quad (15)$$

Priors for Link Probabilities

Similarly, the elements of link probability matrix \mathbf{P} may be given a simple uniform prior over $[0, 1]$:

$$f(p_{ij}) = 1 \quad 0 \leq p_{ij} \leq 1. \quad (16)$$

As there may be some regularity in the values of the link probabilities, we also tried a beta prior:

$$f(p_{ij}|\alpha, \beta) = \frac{1}{B(\alpha, \beta)} p_{ij}^{\alpha-1} (1 - p_{ij})^{\beta-1}, \quad (17)$$

where $B(\alpha, \beta)$ is the beta function,

$$B(\alpha, \beta) = \int_0^1 t^{\alpha-1} (1-t)^{\beta-1} dt. \quad (18)$$

The parameters α and β control the shape of the distribution, which may be convex, concave, or skewed toward 0 or 1. When $\alpha = \beta = 1$, the beta prior becomes a uniform distribution.

We use α and β exponential hyperpriors with mean 1:

$$f(\alpha) = e^{-\alpha} \quad \alpha \geq 0, \quad (19)$$

$$f(\beta) = e^{-\beta} \quad \beta \geq 0. \quad (20)$$

Markov-chain Monte Carlo Sampling

For networks of any appreciable size, the number of possible partitions is far too large to enumerate, so we must use a Markov-chain Monte Carlo (MCMC) technique to sample from the posterior distribution. Here we describe the sampling procedure and the details of the Metropolis-Hastings proposal distribution used.

Sampling Procedure

We employ the standard Metropolis-Hastings algorithm to sample from the posterior distribution over partitions and model hyperparameters [56, 57]. The general idea of an MCMC method is to set up a sequence of dependent samples $\theta_1, \theta_2, \dots$ that is guaranteed to converge to a target distribution, in this case the posterior distribution of our model. Starting from the current sample, a change is proposed, drawn from a *proposal distribution* over possible changes, $q(\theta \rightarrow \theta^*)$. This sample is either rejected, in which case the current sample is repeated, or the proposed sample is accepted as the new sample. The Metropolis-Hastings acceptance probability,

$$r(\theta \rightarrow \theta^*) = \min \left\{ 1, \frac{f(\theta^*) q(\theta^* \rightarrow \theta)}{f(\theta) q(\theta \rightarrow \theta^*)} \right\},$$

guarantees that the sequence of samples will converge to the posterior distribution, $f(\theta|D) \propto f(\theta)f(D|\theta)$, the prior times the likelihood.

For the group model, the samples θ consist of hyperparameters for the model variant—the Dirichlet process prior parameter χ and the beta prior parameters α and β —as well as the group count K and assignment vector \mathbf{G} . The link probabilities \mathbf{P} governing links between groups are not included, because the likelihood function would not be compatible between partitions with different values of K . One possible solution to this problem would be to include \mathbf{P} in the sampling procedure, restrict K to a particular number for a particular run, and then appropriately weight runs with different values of K . Another approach is reversible-jump MCMC [58], which appropriately handles a mapping between two different parameter spaces as part of the Metropolis-Hastings proposal ratio. (We tried a reversible-jump scheme, but chains tended to get stuck at local maxima.)

Instead of trying to sample values of \mathbf{P} , we use the *marginal likelihood* of a partition given model hyperparameters—that is, the posterior distribution, conditional on values of α , β , and \mathbf{G} , integrated over all possible values of \mathbf{P} —directly in the Metropolis-Hastings procedure. This is possible because the marginal likelihood of a single partition can be calculated analytically.

For a beta prior over link probabilities, the likelihood of \mathbf{G} , α and β marginalized over all possible values of \mathbf{P} is

$$f(\mathbf{A}|\mathbf{G}, \alpha, \beta) = \int_{\mathbf{P}} f(\mathbf{P}|\alpha, \beta) f(\mathbf{A}|\mathbf{G}, \mathbf{P}) d\mathbf{P} \quad (21)$$

$$= \prod_{i=1}^K \prod_{j=1}^K \int_0^1 \frac{1}{B(\alpha, \beta)} p_{ij}^{\alpha-1} (1-p_{ij})^{\beta-1} p_{ij}^{Y_{ij}} (1-p_{ij})^{Z_{ij}} dp_{ij} \quad (22)$$

$$= \prod_{i=1}^K \prod_{j=1}^K \int_0^1 \frac{1}{B(\alpha, \beta)} p_{ij}^{Y_{ij}+\alpha-1} (1-p_{ij})^{Z_{ij}+\beta-1} dp_{ij} \quad (23)$$

$$= \prod_{i=1}^K \prod_{j=1}^K \frac{B(Y_{ij} + \alpha, Z_{ij} + \beta)}{B(\alpha, \beta)}. \quad (24)$$

Similarly, for a uniform prior over link probabilities, the marginal likelihood of a particular partition is

simply

$$f(\mathbf{A}|\mathbf{G}) = \prod_{i=1}^K \prod_{j=1}^K B(Y_{ij} + 1, Z_{ij} + 1). \quad (25)$$

Proposal Distribution

For the case of uniform priors on partitions and link probabilities, the proposal distribution only allows changes to the partition. With the Dirichlet process prior on partitions and the beta prior on link probabilities, hyperparameters χ , α , and β can also be changed.

The proposal distribution is described as follows:

1. Each hyperparameter h (α , β , and χ) is chosen for update with probability p_h , where p_h are tuned to improve convergence. A proposed new value h' is drawn from a uniform distribution between $\max(0, h - r_h)$ and $h + r_h$, where r_h is a proposal radius manually tuned to improve convergence. (A scale-free proposal could easily be used instead, and may require less tuning.)
2. With probability $(1 - \sum_h p_h)$, a group-change move is proposed:
 - (a) A node i is chosen uniformly at random as the species to be moved.
 - (b) Another node $j \neq i$ is chosen uniformly at random.
 - (c) If i and j are in different groups, node i is moved into the group of node j . If i and j are in the same group, node i is moved into a new group.

Metropolis-coupled MCMC

Although the Metropolis-Hastings algorithm is guaranteed to converge to the target distribution at some point, local maxima in the likelihood surface can cause a chain to become stuck for long periods of time. One approach to avoiding this problem, known as ‘‘Metropolis coupling,’’ involves running multiple chains in parallel. One chain, the ‘‘cold chain,’’ explores the target distribution, while the other chains, ‘‘hot chains,’’ explore low-likelihood configurations more freely. Periodically, swaps are proposed between chains, allowing good configurations discovered on hot chains to propagate toward the cold chain.

Rather than exploring the target distribution $f(\theta|D) \propto f(\theta)f(D|\theta)$, heated chains explore

$$f_\tau(\theta|D) \propto f(\theta) [f(D|\theta)]^\tau \quad \tau \in [0, 1], \quad (26)$$

where τ is a heating parameter. We use linearly spaced values of τ , with the hottest chain exploring the prior ($\tau = 0$) and the coldest chain exploring the posterior ($\tau = 1$).

Swap moves are standard Metropolis-Hastings proposals, but rather than considering a change to a single chain, they consider a change to the joint distribution of two chains. The acceptance probability is thus the ratio of the joint distribution after and before the move:

$$r((\theta_i, \theta_j) \rightarrow (\theta_j, \theta_i)) = \frac{f(\theta_j) [f(D|\theta_j)]^{\tau_i} f(\theta_i) [f(D|\theta_i)]^{\tau_j}}{f(\theta_i) [f(D|\theta_i)]^{\tau_i} f(\theta_j) [f(D|\theta_j)]^{\tau_j}} \quad (27)$$

$$= \left[\frac{f(D|\theta_i)}{f(D|\theta_j)} \right]^{\tau_j - \tau_i}, \quad (28)$$

where θ_i, θ_j are the configurations that begin in chains i and j , and τ_i, τ_j are the heat parameters of the two chains.

The use of multiple heated chains has the side effect of drastically improving estimates of marginal likelihoods for model selection, as described in the next section.

Model Selection via Marginal Likelihood

The marginal likelihood of a model is the likelihood averaged over the prior distribution. That is, it is the likelihood one would expect by randomly sampling parameters from the prior distribution:

$$f(D|M) = \int_{\theta} f(\theta)f(D|\theta) d\theta. \quad (29)$$

This value serves as a useful measure of model fit because it directly incorporates the dependence of the likelihood on uncertainty in parameter values, implicitly penalizing extra degrees of freedom [49]. If an additional parameter improves the maximum likelihood but decreases the average likelihood, the model suffers from overfitting relative to the simpler model.

Marginal Likelihood for the Group Model

The marginal likelihood for the group model involves integrating over all hyperparameters, partitions, and link probabilities. For the model with uniform distributions over partitions and link probabilities, the marginal likelihood is

$$f(\mathbf{A}|M_{u,u}) = \sum_{\mathbf{G}} f(\mathbf{G})f(\mathbf{A}|\mathbf{G}) \quad (30)$$

$$= \sum_{\mathbf{G}} \frac{1}{\mathcal{B}(N)} \left[\prod_{i=1}^K \prod_{j=1}^K B(Y_{ij} + 1, Z_{ij} + 1) \right]. \quad (31)$$

With a Dirichlet process prior over partitions and a uniform distribution over link probabilities, the marginal likelihood is similarly

$$f(\mathbf{A}|M_{d,u}) = \int_0^{\infty} f(\chi) \sum_{\mathbf{G}} f(\mathbf{G}|\chi)f(\mathbf{A}|\mathbf{G}) d\chi. \quad (32)$$

Using a uniform prior over partitions and a beta prior over link probabilities yields

$$f(\mathbf{A}|M_{u,b}) = \sum_{\mathbf{G}} f(\mathbf{G}) \int_0^{\infty} f(\alpha) \int_0^{\infty} f(\beta)f(\mathbf{A}|\mathbf{G}, \alpha, \beta) d\beta d\alpha. \quad (33)$$

Combining both gives

$$f(\mathbf{A}|M_{d,b}) = \int_0^{\infty} f(\chi) \sum_{\mathbf{G}} f(\mathbf{G}|\chi) \int_0^{\infty} f(\alpha) \int_0^{\infty} f(\beta)f(\mathbf{A}|\mathbf{G}, \alpha, \beta) d\beta d\alpha d\chi. \quad (34)$$

Thermodynamic Integration for Marginal Likelihood Estimation

As enumeration across all possible partitions is impossible for networks of any significant size, we would like to use MCMC to estimate the marginal likelihood for the sake of comparison among different models. Marginal likelihood estimates derived from a single chain, such as the harmonic mean estimator of Raftery [31], converge very slowly, because MCMC fails to sample sufficiently from low-likelihood areas. However, it is possible to use the information gathered about low-likelihood areas in heated chains using a technique called thermodynamic integration [59, 60], or path sampling [61].

Assuming a continuum of heated chains, the thermodynamic estimator for the log-marginal likelihood

is

$$\log \hat{\mathcal{L}}(M) = \int_0^1 \frac{1}{m} \sum_{i=1}^m \pi(\theta_{i,\tau}) \log \mathcal{L}(\theta_{i,\tau}) d\tau \quad (35)$$

where m is the number of samples in the MCMC output, and $\theta_{i,\tau}$ is a single sample from the output in a chain with heat parameter τ [60]. With a finite number of chains, we estimate this integral using cubic spline interpolation as implemented in the `splinefun` function in the R software package [62].

Consensus Partitions

The full output of an MCMC chain from the group model includes an extremely large number of different partitions, and, for the sake of interpretation, it is desirable to seek a *consensus partition* that does a reasonable job of summarizing the distribution. We use a simple, computationally inexpensive method to accomplish this task: in short, clustering the nodes in the network based on a pairwise group-membership matrix.

The group-membership matrix \mathbf{M} is the posterior probability that two nodes are in the same group and 0 otherwise, that is,

$$\mathbf{M} = \sum_{\mathbf{G}} P(\mathbf{G}|\mathbf{A}) \mathbf{M}_{\mathbf{G}}, \quad (36)$$

where an entry $\mathbf{M}_{\mathbf{G}}$ is 1 if nodes i and j are in the same group, that is,

$$\mathbf{M}_{\mathbf{G},ij} = \delta_{\mathbf{G}_i, \mathbf{G}_j}, \quad (37)$$

where δ is the Kronecker delta and \mathbf{G} is the assignment vector for the partition. This matrix is estimated from MCMC output as the fraction of MCMC samples in which the corresponding species are in the same group:

$$\hat{\mathbf{M}} = \frac{1}{N} \sum_{i=1}^N \mathbf{M}_{\mathbf{G}_i}. \quad (38)$$

A consensus partition is formed by applying a hierarchical clustering algorithm to the group-membership matrix estimate $\hat{\mathbf{M}}$, and then cutting the dendrogram at some number of groups K , forming a consensus partition with assignment vector \mathbf{G}_K and group-membership matrix \mathbf{M}_K . The goodness of fit of a consensus partition is simply measured as the correlation between $\hat{\mathbf{M}}$ and \mathbf{M}_K . The best consensus partition is thus identified using the value of K that gives the highest correlation.

We use the average-linkage clustering algorithm [63] as implemented by the `hclust` function in the R software package [62], treating $\mathbf{1} - \hat{\mathbf{M}}$ as distance matrix. We find that the average-linkage algorithm produces higher correlations than the other algorithms implemented as well as ideal K close to the mean K in the MCMC output. Furthermore, we find that consensus partitions produce higher correlations with the $\hat{\mathbf{M}}$ than any individual partition in the MCMC output.

Acknowledgments

We acknowledge the support of NSF grant EF-0827493 (Program on Theory in Biology) to S.A. and M.P., and of the DOE Computational Science Graduate Fellowship (grant DE-FG02-97ER25308) to E.B. T.B. was supported by the Howard Hughes Medical Institute, and M.P. is a Howard Hughes Medical Institute Investigator.

A.D. acknowledges the McDonnell Foundation for financial support, the Frankfurt Zoological Society for logistical support in the Serengeti for his work on food webs, and the members of Serengeti Biocomplexity Project for many interesting discussions about the Serengeti food web.

The funders had no role in study design, data collection and analysis, decision to publish, or preparation of the manuscript.

References

1. Cohen JE (1995) *Frontiers in Mathematical Biology*, Springer, volume 100 of Lecture Notes in Biomathematics. pp. 351–380.
2. Camerano L (1880) Dell'equilibrio dei viventi merce la reciproca distruzione. *Accademia delle Scienze di Torino* 15: 393–414.
3. Elton CS (1927) *Animal Ecology*. Text-Books of Animal Biology. London: Sidgwick & Jackson, Ltd.
4. May RM (1973) *Stability and Complexity in Model Ecosystems*. Princeton University Press.
5. Pimm S, Lawton J (1980) Are food webs divided into compartments? *The Journal of Animal Ecology* 49: 879–898.
6. Krause A, Frank K, Mason D, Ulanowicz R, Taylor W (2003) Compartments revealed in food-web structure. *Nature* 426: 282–285.
7. Guimera R, Stouffer D, Sales-Pardo M, Leicht E, Newman M, et al. (2010) Origin of compartmentalization in food webs. *Ecology* 91: 2941–2951.
8. Allesina S, Pascual M (2009) Food web models: a plea for groups. *Ecology Letters* 12: 652–62.
9. Girvan M, Newman M (2002) Community structure in social and biological networks. *Proceedings of the National Academy of Sciences* 99: 7821.
10. Burns T (1989) Lindeman's contradiction and the trophic structure of ecosystems. *Ecology* 70: 1355–1362.
11. Luczkovich JJ, Borgatti SP, Johnson JC, Everett MG (2003) Defining and measuring trophic role similarity in food webs using regular equivalence. *Journal of Theoretical Biology* 220: 303–321.
12. Cohen JE, Briand F, Newman CM (1990) *Community Food Webs: Data and Theory*. Biomathematics. Springer.
13. Williams R, Martinez N (2000) Simple rules yield complex food webs. *Nature* 404: 180–183.
14. Allesina S, Alonso D, Pascual M (2008) A general model for food web structure. *Science* 320: 658–61.
15. McCarthy MA (2007) *Bayesian Methods for Ecology*. Cambridge University Press.
16. Hoff P, Raftery A, Handcock M (2002) Latent space approaches to social network analysis. *Journal of the American Statistical Association* 97: 1090–1098.
17. Park Y, Moore C, Bader JS (2010) Dynamic networks from hierarchical Bayesian graph clustering. *PLoS One* 5: e8118.

18. Clauset A, Moore C, Newman MEJ (2008) Hierarchical structure and the prediction of missing links in networks. *Nature* 453: 98–101.
19. Williams R, Anandanadesan A, Purves D (2010) The probabilistic niche model reveals the niche structure and role of body size in a complex food web. *PLoS One* 5: e12092.
20. Yang Z, Rannala B (1997) Bayesian phylogenetic inference using DNA sequences: a Markov chain Monte Carlo method. *Molecular Biology and Evolution* 14: 717.
21. Mau B, Newton M, Larget B (1999) Bayesian phylogenetic inference via Markov chain Monte Carlo methods. *Biometrics* 55: 1–12.
22. Dobson A (2009) Food-web structure and ecosystem services: insights from the Serengeti. *Philosophical Transactions of the Royal Society B: Biological Sciences* 364: 1665–1682.
23. Sinclair ARE, Norton-Griffiths M, editors (1979) *Serengeti, Dynamics of an Ecosystem*. University Of Chicago Press.
24. Sinclair ARE, Arcese P, editors (1995) *Serengeti II: Dynamics, Management, and Conservation of an Ecosystem*. University Of Chicago Press.
25. Sinclair ARE, Packer C, Mduma SA, Fryxell JM, editors (2008) *Serengeti III: Human Impacts on Ecosystem Dynamics*. University Of Chicago Press.
26. McNaughton S (1983) Serengeti grassland ecology: the role of composite environmental factors and contingency in community organization. *Ecological Monographs* 53: 291–320.
27. Wang Y, Wong G (1987) Stochastic blockmodels for directed graphs. *Journal of the American Statistical Association* 82: 8–19.
28. Ferguson T (1973) A Bayesian analysis of some nonparametric problems. *The Annals of Statistics* 1: 209–230.
29. Jeffreys H (1935) Some tests of significance, treated by the theory of probability. *Proceedings of the Cambridge Philosophical Society* 31: 203–222.
30. Jeffreys H (1961) *Theory of Probability*. The International Series of Monographs on Physics. Oxford: Clarendon Press, 3rd edition.
31. Kass R, Raftery A (1995) Bayes factors. *Journal of the American Statistical Association* 90.
32. Burnham KP, Anderson D (2002) *Model Selection and Multi-Model Inference*. Springer.
33. Sinclair A, Mduma S, Brashares J (2003) Patterns of predation in a diverse predator–prey system. *Nature* 425: 288–290.
34. Casebeer R, Koss G (1970) Food habits of wildebeest, zebra, hartebeest and cattle in Kenya Masailand. *African Journal of Ecology* 8: 25–36.
35. Cooper S, Holekamp K, Smale L (1999) A seasonal feast: long-term analysis of feeding behaviour in the spotted hyaena (*Crocuta crocuta*). *African Journal of Ecology* 37: 149–160.
36. Hansen R, Mugambi M, Bauni S (1985) Diets and trophic ranking of ungulates of the northern Serengeti. *The Journal of Wildlife Management* : 823–829.
37. Murray M (1993) Comparative nutrition of wildebeest, hartebeest and topi in the Serengeti. *African Journal of Ecology* 31: 172–177.

38. Talbot L, Talbot M (1962) Food preferences of some East African wild ungulates. *East African Agricultural and Forestry Journal* 27: 131–138.
39. Talbot LM, Talbot MH (1963) The Wildebeest in Western Masailand, East Africa. *Wildlife Monographs* : 3–88.
40. Schaller G (1972) *The Serengeti Lion*. University of Chicago Press.
41. Caro T (1994) *Cheetahs of the Serengeti Plains: Group Living in an Asocial Species*. University of Chicago Press.
42. Kruuk H (1972) *The Spotted Hyaena*. University of Chicago Press.
43. McNaughton S (1985) Ecology of a grazing ecosystem: the Serengeti. *Ecological Monographs* 55: 259–294.
44. Vesey-FitzGerald D (1960) Grazing succession among East African game animals. *Journal of Mammalogy* 41: 161–172.
45. Lamprecht J (1978) On diet, foraging behaviour and interspecific food competition of jackals in the Serengeti National Park, East Africa. *Zeitschrift für Säugetierkunde* 43: 210–223.
46. Rooney N, McCann K, Moore J (2008) A landscape theory for food web architecture. *Ecology Letters* 11: 867–881.
47. McCann K, Rasmussen J, Umbanhowar J (2005) The dynamics of spatially coupled food webs. *Ecology Letters* 8: 513–523.
48. Rezende E, Albert E, Fortuna M, Bascompte J (2009) Compartments in a marine food web associated with phylogeny, body mass, and habitat structure. *Ecology Letters* 12: 779–788.
49. Bolker BM (2008) *Ecological Models and Data in R*. Princeton University Press.
50. Good B, De Montjoye Y, Clauset A (2010) Performance of modularity maximization in practical contexts. *Physical Review E* 81: 46106.
51. Newman M (2006) Modularity and community structure in networks. *Proceedings of the National Academy of Sciences* 103: 8577.
52. Jeong H, Tombor B, Albert R, Oltvai Z, Barabási A (2000) The large-scale organization of metabolic networks. *Nature* 407: 651–654.
53. Bascompte J, Jordano P, Melián C, Olesen J (2003) The nested assembly of plant–animal mutualistic networks. *Proceedings of the National Academy of Sciences* 100: 9383.
54. Huelsenbeck JP, Suchard MA (2007) A nonparametric method for accommodating and testing across-site rate variation. *Systematic Biology* 56: 975–87.
55. Xing E, Jordan M, Sharan R (2007) Bayesian haplotype inference via the Dirichlet process. *Journal of Computational Biology* 14: 267–284.
56. Metropolis N, Rosenbluth A, Rosenbluth M, Teller A, Teller E (1953) Equation of state calculations by fast computing machines. *Journal of Chemical Physics* 21: 1087.
57. Hastings W (1970) Monte Carlo sampling methods using Markov chains and their applications. *Biometrika* 57: 97–109.

58. Green P (1995) Reversible jump Markov chain Monte Carlo computation and Bayesian model determination. *Biometrika* 82: 711.
59. Lartillot N, Philippe H (2006) Computing Bayes factors using thermodynamic integration. *Systematic Biology* 55: 195–207.
60. Beerli P, Palczewski M (2010) Unified framework to evaluate panmixia and migration direction among multiple sampling locations. *Genetics* 185: 313–26.
61. Gelman A, Meng X (1998) Simulating normalizing constants: from importance sampling to bridge sampling to path sampling. *Statistical Science* 13: 163–185.
62. R Development Core Team (2010) R: A Language and Environment for Statistical Computing. R Foundation for Statistical Computing, Vienna, Austria. URL <http://www.R-project.org>. ISBN 3-900051-07-0.
63. Sokal R, Michener C (1958) A statistical method for evaluating systematic relationships. *University of Kansas Science Bulletin* 38: 1409–1438.
64. Duong T (2007) ks: Kernel density estimation and kernel discriminant analysis for multivariate data in R. *Journal of Statistical Software* 21: 1–16.

Figures

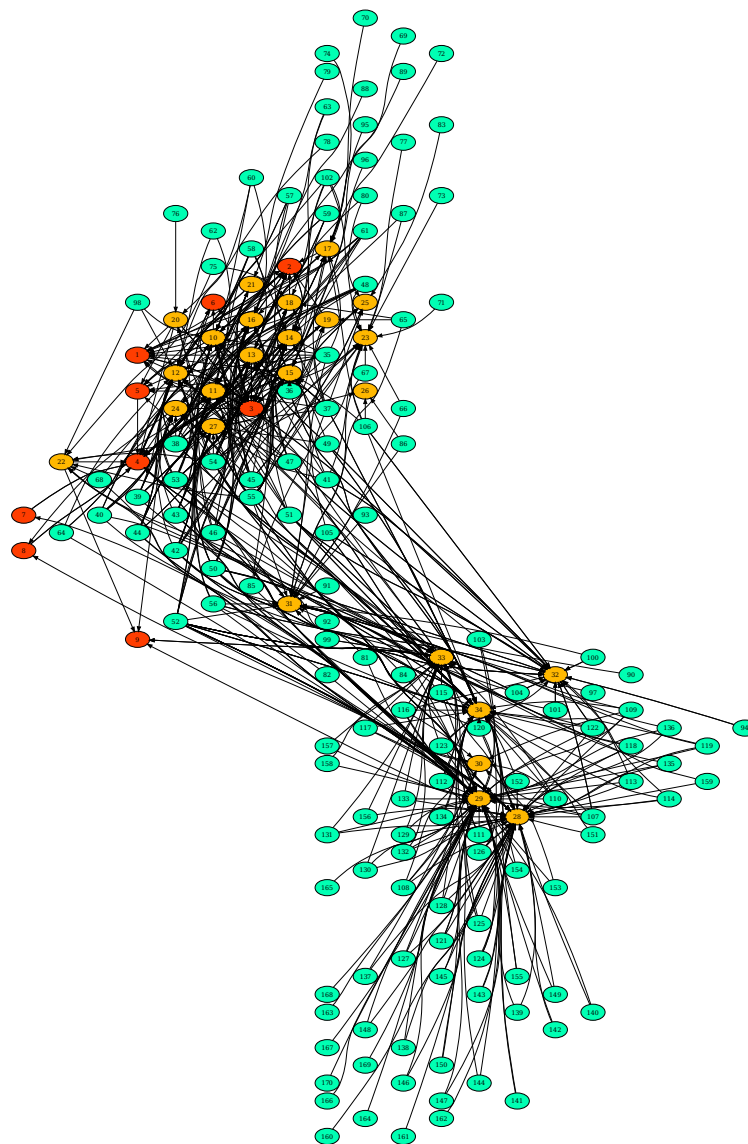


Figure 1. The Serengeti food web. The network is shown using a spring-layout algorithm without clustering. Plant, herbivore, and carnivore nodes are green, orange, and red, respectively.

Supporting Information

(See supporting file `tab_S1_species_list.csv` for data.)

Table S1. Species in the Serengeti food web.

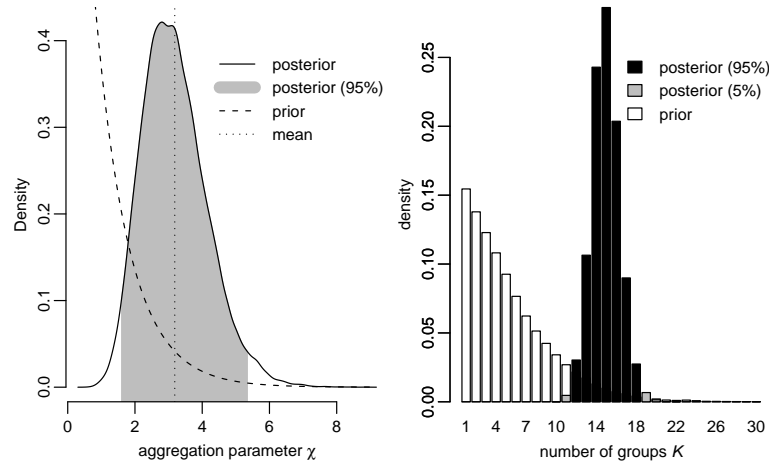


Figure 2. Posterior distributions and prior expectations of aggregation parameter χ and group count K .

(See supporting file `tab_S2_edge_list.csv` for data.)

Table S2. Feeding links in the Serengeti food web.

(See supporting file `tab_S3_consensus_partition.csv` for data.)

Table S3. 16-group consensus partition.

(See supporting file `tab_S4_link_density.csv` for data.)

Table S4. Link densities between groups in the 16-group consensus partition.

Tables

Table 1. Marginal likelihood estimates for model variants calculated via thermodynamic integration.

Partition prior	Link prior	Log marginal likelihood estimate	95% bootstrap confidence int.
Uniform	Uniform	-1826.87	(-1826.94, -1826.82)
Uniform	Beta	-1463.22	(-1463.39, -1463.03)
Dirichlet process	Uniform	-1547.41	(-1547.45, -1547.37)
Dirichlet process	Beta	-1356.96	(-1357.02, -1356.90)
One group	Uniform	-2870.58	(exact)
170 groups	Uniform	-20031.95	(exact)
170 groups	Beta	-2870.58	(exact)

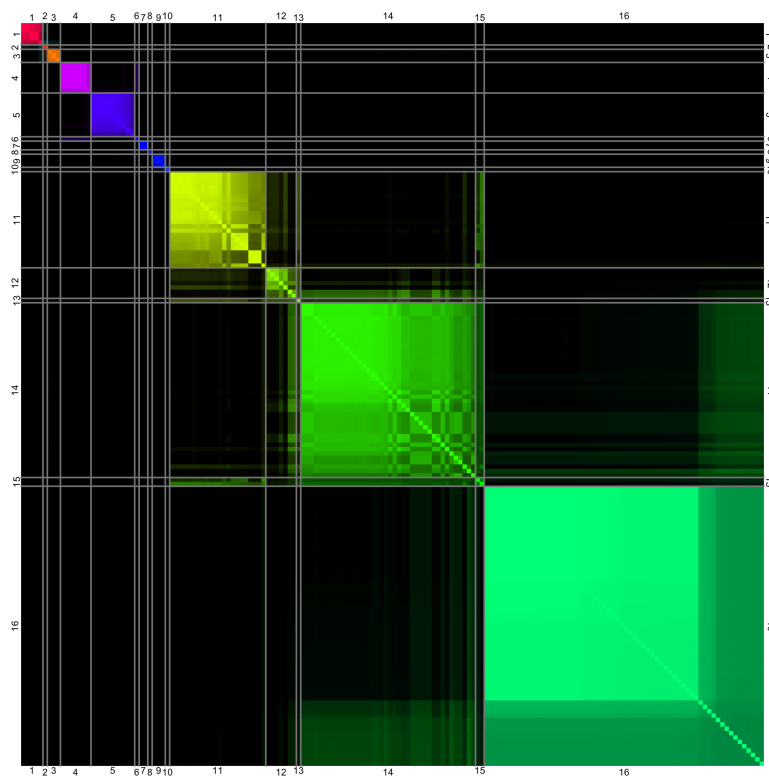


Figure 3. Pairwise group membership matrix. Species are identically ordered top to bottom and left to right according to the 16-group consensus partition as listed in Table 2. Hue indicates group identity; color saturation indicates the fraction of partitions in which species occupy the same group. Note that this image conveys information about group membership, not network connectivity.

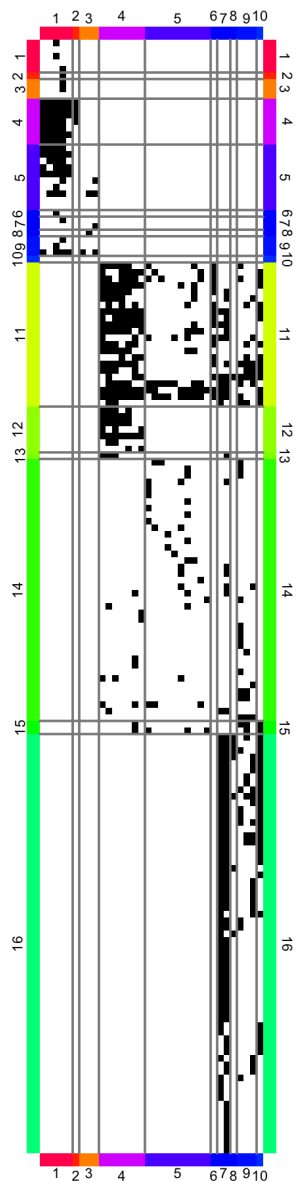


Figure 4. Adjacency matrix ordered by groups. Species are identically ordered top to bottom and left to right according to the 16-group consensus partition as listed in Table 2. Black matrix entries indicate that the species in the column feeds on the species in the row. Columns that would indicate prey of plant groups are omitted. Note that in a modular network according to the standard definition, links would be concentrated on the diagonal of the adjacency matrix, since they occur within groups. By contrast, here links are concentrated in off-diagonal blocks.

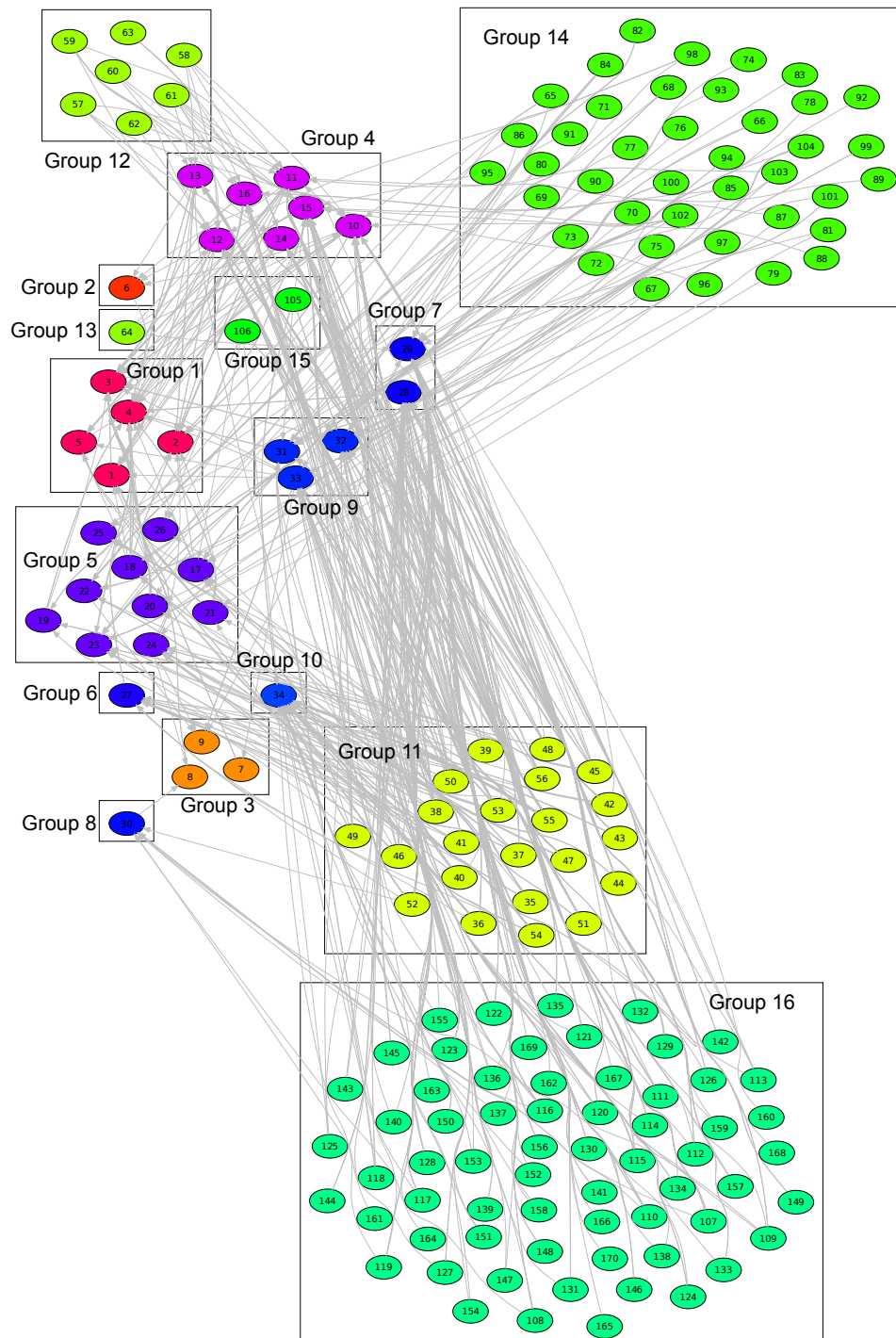


Figure 5. Network layout of groups. The network is shown organized and colored by group according to the 16-group consensus partition listed in Table 2.

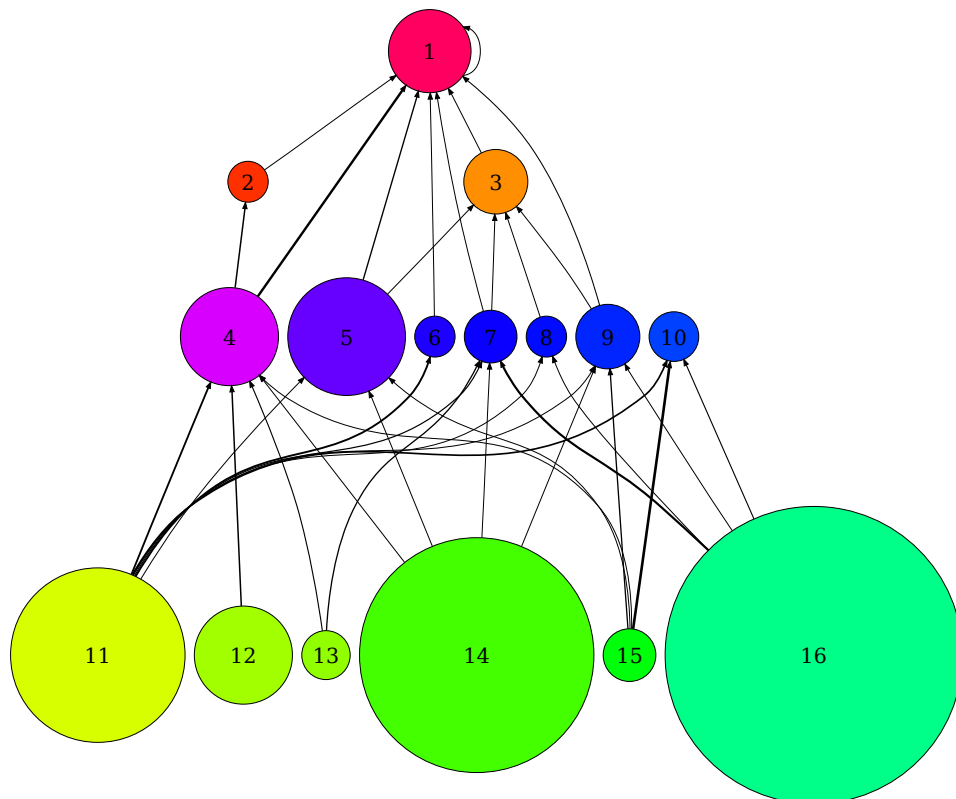


Figure 6. Network layout of aggregated groups. Nodes in the network are aggregated and colored by group according to the 16-group consensus partition listed in Table 2, and arranged vertically by trophic level. Line thickness indicates the link density between groups. Node area is proportional to the number of species in a group.

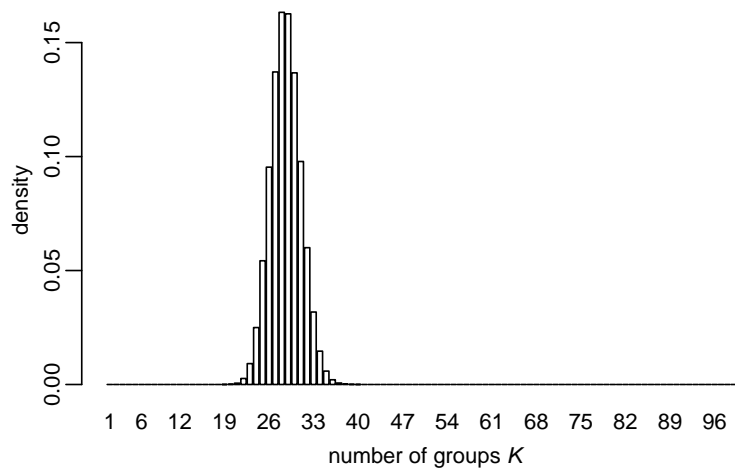


Figure S1. Implicit prior on number of groups with uniform partition prior. The prior distribution on number of groups K is shown for a uniform partition prior for a network with 100 nodes. The mode of the distribution is at $K = 28$.

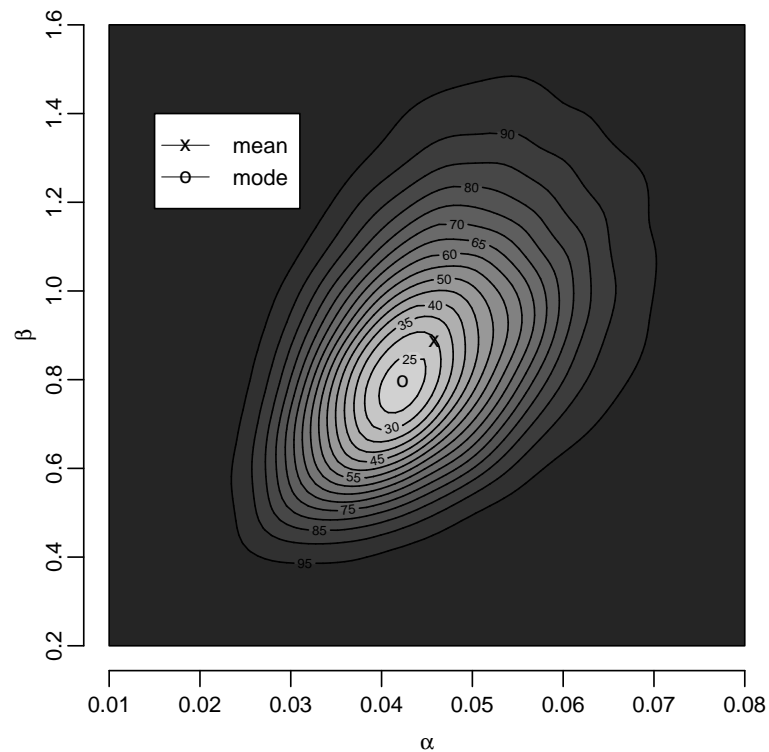


Figure S2. Posterior distributions of link density parameters α and β . Color brightness indicates posterior density, estimated using the ks multivariate kernel density estimation package for R [64]. Contours indicate cumulative density. The α parameter is significantly lower than 1, indicating departure from a uniform distribution.

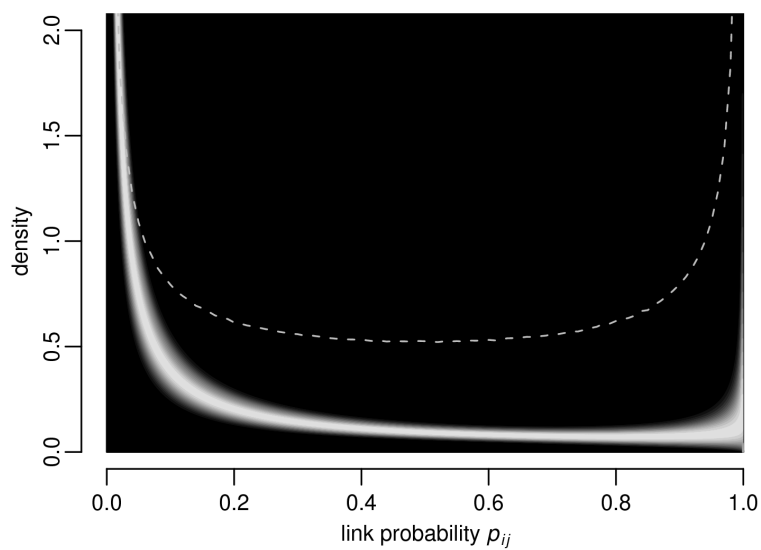


Figure S3. Distribution of link probability parameters. The prior distribution for link probability parameters, integrated over the priors for beta distribution parameters α and β , is indicated with a dotted line. The heat map shows beta distributions corresponding to the posterior distribution for α and β , with lightness indicating the posterior density of the parameter values.

Table 2. Groups identified in the Serengeti food web using a 16-group consensus partition.

Group 1	<i>Crocuta crocuta</i> , <i>Lycaon pictus</i> , <i>Panthera leo</i> , <i>Panthera pardus</i> , <i>Acinonyx jubatus</i>
Group 2	<i>Canis aureus</i>
Group 3	<i>Canis mesomelas</i> , <i>Leptailurus serval</i> , <i>Caracal caracal</i>
Group 4	<i>Connochaetus taurinus</i> , <i>Gazella granti</i> , <i>Gazella thomsoni</i> , <i>Equus burchelli</i> , <i>Alcelaphus buselaphus</i> , <i>Aepyceros melampus</i> , <i>Damaliscus korrigum</i>
Group 5	<i>Kobus ellipsiprymnus</i> , <i>Phacochaerus aethiopicus</i> , <i>Tragelaphus scriptus</i> , <i>Ourebia ourebi</i> , <i>Redunca redunca</i> , <i>Pedetes capensis</i> , <i>Taurotragus oryx</i> , <i>Rhabdomys pumilio</i> , <i>Hippopotamus amphibius</i> , <i>Cercopithecus aethiops</i>
Group 6	<i>Syncerus caffer</i>
Group 7	<i>Heterohyrax brucei</i> , <i>Procavia capensis</i>
Group 8	<i>Agama planiceps</i>
Group 9	<i>Papio anubis</i> , <i>Giraffa camelopardalis</i> , <i>Madoqua kirkii</i>
Group 10	<i>Loxodonta africana</i>
Group 11	<i>Panicum coloratum</i> , <i>Sporobolus pyramidalis</i> , <i>Hyparrhenia filipendula</i> , <i>Harpachne schimperii</i> , <i>Digitaria macroblephara</i> , <i>Eragrostis tenuifolia</i> , <i>Grewia bicolor</i> , <i>Aristida adoensis</i> , <i>Brachiaria semiundulata</i> , <i>Pennisetum mezianum</i> , <i>Bothriochloa insculpta</i> , <i>Panicum maximum</i> , <i>Sida</i> spp., <i>Eustachys paspaloides</i> , <i>Croton macrostachyus</i> , <i>Solanum incanum</i> , <i>Indigofera hochstetteri</i> , <i>Hibiscus</i> spp., <i>Heteropogon contortus</i> , <i>Cynodon dactylon</i> , <i>Themeda triandra</i> , <i>Balanites aegytiaca</i>
Group 12	<i>Digitaria scalarum/abysinnica</i> , <i>Dinebra retroflexa</i> , <i>Ischaemum afrum</i> , <i>Eragrostis cilianensis</i> , <i>Hyparrhenia rufa</i> , <i>Sporobolus fimbriatus</i> , <i>Sporobolus spicatus</i>
Group 13	<i>Microchloa kunthii</i>
Group 14	<i>Echinochloa haploclada</i> , <i>Digitaria milanjiana</i> , <i>Panicum deustum</i> , <i>Digitaria ternata</i> , <i>Andropogon schirensis</i> , <i>Cymbopogon excavatus</i> , <i>Setaria sphacelata</i> , <i>Typha capensis</i> , <i>Setaria pallidifusca</i> , <i>Phragmites mauritianus</i> , <i>Eragrostis exasperata</i> , <i>Andropogon greenwayi</i> , <i>Lonchocarpus ericalyx</i> , <i>Sporobolus centrifugus</i> , <i>Hyparrhenia dissoluta</i> , <i>Chloris roxburghiana</i> , <i>Aristida hordacea</i> , <i>Chloris pycnothrix</i> , <i>Panicum repens</i> , <i>Aristida kenyensis</i> , <i>Combretum molle</i> , <i>Acacia xanthophloea</i> , <i>Disperma kilimandscharica</i> , <i>Vossia cuspidata</i> , <i>Odyssea jaegeri</i> , <i>Sporobolus ioclados</i> , <i>Euphorbia candelabrum</i> , <i>Sorghum versicolor</i> , <i>Kigelia africana</i> , <i>Olea</i> spp., <i>Sporobolus festivus</i> , <i>Acacia pallens</i> , <i>Crotalaria spinosa</i> , <i>Digitaria diagonalis</i> , <i>Boscia augustifolia</i> , <i>Acacia robusta</i> , <i>Acacia seyal/hockii</i> , <i>Chloris gayana</i> , <i>Pennisetum stramineum</i> , <i>Commiphora africana/trothae</i>
Group 15	<i>Acacia senegal</i> , <i>Acacia tortilis</i>
Group 16	<i>Grewia fallax</i> , <i>Cissus quadrangularis</i> , <i>Cissus rotundifolia</i> , <i>Commelina africana</i> , <i>Allophylus rubifolus</i> , <i>Sensevieria ehrenbergiana</i> , <i>Pavetta assimilis</i> , <i>Phyllanthus sepialis</i> , <i>Acalypha fruticosa</i> , <i>Maerua triphllya</i> , <i>Ficus glumosa</i> , <i>Croton dichogamus</i> , <i>Sclerocarya birrea</i> , <i>Capparis tomentosa</i> , <i>Ximenia caffra</i> , <i>Cordia ovalis</i> , <i>Grewia trichocarpa</i> , <i>Abutilon angulatum</i> , <i>Pappaea capensis</i> , <i>Commiphora schimperii</i> , <i>Albuca</i> spp., <i>Ficus ingens</i> , <i>Hoslundia opposita</i> , <i>Ocinum suave</i> , <i>Cenchrus ciliaris</i> , <i>Solanum dennekense</i> , <i>Aloe macrosiphon</i> , <i>Indigofera basiflora</i> , <i>Ipomoea obscura</i> , <i>Albizia harveyi</i> , <i>Ficus thinningii</i> , <i>Emilia coccinea</i> , <i>Cyphostemma nierensis</i> , <i>Spirocarpa</i> spp., <i>Sensevieria suffruticosa</i> , <i>Pupalia lappacea</i> , <i>Aloe secundiflora</i> , <i>Turreae fischeri</i> , <i>Pavonia patens</i> , <i>Jasminum fluminense</i> , <i>Acacia clavigera</i> , <i>Cassia didymobotrya</i> , <i>Kedrotis foetidissima</i> , <i>Hypoestes forskalii</i> , <i>Zisiphus mucronata</i> , <i>Commiphora merkeri</i> , <i>Blepharis acanthoides</i> , <i>Iboza</i> sp., <i>Rhoicissus revouillii</i> , <i>Kalanchoe</i> sp., <i>Solanum nigrum</i> , <i>Achyranthes aspera</i> , <i>Digitaria velutina</i> , <i>Tricholaena eichingeri</i> , <i>Lippia ukambensis</i> , <i>Heliotropium steudneri</i> , <i>Kyllinga nervosa</i> , <i>Sporobolus stapfianus</i> , <i>Cyperus kilimandscharica</i> , <i>Pellaea calomelanos</i> , <i>Sporobolus pellucidus</i> , <i>Eragrostis aspera</i> , <i>Eriochloa nubica</i> , <i>Diheteropogon amplexus</i>